An Attached Flow Design of a Noninterfering Leading-Edge Extension to a Thick Delta Wing

Farhad Ghaffari*
Vigyan Research Associates, Inc., Hampton, Virginia
and
John E. Lamar†
NASA Langley Research Center, Hampton, Virginia

An analytical procedure for the determination of the shape of leading-edge extension (LEE) that satisfies design criteria, including especially noninterference at the wing design point, has been developed for thick delta wings. The LEE device best satisfying all criteria is designed to be mounted on a wing along a dividing stream surface associated with an attached flow design lift coefficient ($C_{L,d}$) of greater than zero. This device is intended to impove the aerodynamic performance of transonic aircraft at $C_L > C_{L,d}$ by controlling the wing flowfield with the vortex system emanating from the LEE leading edge. In order to quantify this process, a twisted and cambered thick delta wing was chosen for the initial application of this design procedure. Appropriate computer codes representing potential and vortex flows were employed to determine the dividing stream surface at $C_{L,d}$ and an optimized LEE planform shape at $C_L > C_{L,d}$, respectively. To aid in the LEE selection, the aerodynamic effectiveness of 36 planforms was investigated at $C_L > C_{L,d}$. This study showed that reducing the span of the candidate LEEs has the most detrimental effect on the overall aerodynamic efficiency, regardless of the shape or area. Furthermore, for a fixed area, constant-chord LEE candidates were relatively more efficient than those with sweep less than the wing. At $C_{L,d}$, the presence of the LEE planform best satisfying the design criteria was found to have no effect on the wing-alone aerodynamic performance.

Nomenclature

A = aspect ratio of wing
b = span
C_D = drag coefficient, drag/$q_\infty S$
C_L = lift coefficient, lift/$q_\infty S$
C_m = pitching moment coefficient, pitching moment/$q_\infty S\bar{c}$
C_p = pressure coefficient, $(p-p_\infty)/q_\infty$
ΔC_p = lifting pressure coefficient, $C_{p,u}-C_{p,l}$
c = chord
$\bar{c}$ = reference chord
FVS = free vortex sheet
L/D = lift-to-drag ratio
LEE = leading-edge extension
M_∞ = freestream Mach number
p = static pressure
p_∞ = freestream static pressure
PAN AIR = panel aerodynamics computer code
PSS = pseudo-stagnation streamline
PSSS = pseudo-stagnation stream surface
q_∞ = freestream dynamic pressure
S = wing reference area
V_X, V_Y, V_Z = X, Y, and Z components of the total velocity, respectively
VLM-SA = vortex lattice method coupled with suction analogy
X, Y, Z = coordinate axes centered at the leading-edge apex
$\bar{x}/c$ = fractional distance along the local chord of the called out surface
α = angle of attack, deg
η = fraction of wing theoretical semispan ($b_T/2 = 16.77$ in.)
η_{LEE} = b_{LEE}/b_w
Λ = leading-edge sweep angle, deg

Subscripts

d = design
l = lower surface
LEE = leading-edge extension
r = root
T = theory
u = upper surface
w = wing
0 = value at $C_L = 0.0$

Introduction

FUTURE swept-wing aircraft capable of cruising at high subsonic or supersonic speeds are likely to be required to operate efficiently over an extended portion of their flight envelope. There are two basic approaches to designing such aircraft. The first is a conventional approach that seeks to maintain fully attached flow at each point of the envelope. The second approach attempts to use the organized separated flow at conditions which are off-design and attached flow at design. The design criterion of the conventional approach is more desirable, because an aerodynamically efficient aircraft always achieves its best performance with attached flow unless the wing is extremely slender. The primary cause of this high efficiency is the production of aerodynamic thrust associated with attached flow at the leading edge. In order to maintain attached flow on such swept wings, techniques such as variable camber at the leading edge, a leading-edge flap, and large leading-edge radii have been developed. These techniques, illustrated in Fig. 1a via streamwise wing cuts, have been known for their potential to delay the onset of the leading-edge flow separation on moderate swept wings.[1-3] However, the natural tendency of flow toward separation for highly swept wings, especially at off-design conditions such as takeoff, landing, and maneuvering, appears inevitable. At off-design performance, the flow characteristics of such aircraft are changed

Presented as Paper 85-0350 at the AIAA 23rd Aerospace Sciences Meeting, Reno, NV, Jan. 14-17, 1985; received June 16, 1985; revision received Nov. 12, 1985. This paper is declared a work of the U.S. Government and therefore is in the public domain.

*Research Engineer. Member AIAA.
†Senior Research Scientist. Associate Fellow AIAA.

dramatically by the formation of a generally stable and coherent leading-edge vortex system. The schematic flow representation at off-design condition is shown by a streamwise cut (Fig. 1b) for blunt leading-edge swept wings. The resultant vortex system generates additional lift, caused by low-pressure regions under the stable vortex system, and produces the well-known nonlinear aerodynamic behavior called "vortex lift." Accompanying the additional lift is the increased drag that results from the loss of the leading-edge suction associated with attached flow around the leading edge.[4] This drag increase restricts subsonic and transonic sustained maneuvering because of the excess engine thrust required. Furthermore, with increasing angle of attack, the shed vortex system has an inboard movement of its center and may fail to reattach on the wing and/or experience breakdown. The latter two phenomena result in a pitch-up pitching moment.[5]

As the technology in aircraft design has developed, methods for improving multimission capability have been explored. One such method, the subject of this study, is to design the wing to achieve fully attached flow at the cruise design condition and controlled leading-edge separation at takeoff, landing, and maneuvering.[3] This method is an alternative approach to the conventional attached flow approach for designing a high-subsonic and supersonic cruise swept-wing aircraft. The basic concept of this alternative approach is to let the flow separate and roll up into an organized leading-edge vortex system, which is located appropriately. For this purpose, a family of vortex control devices, such as fixed (i.e., sharp leading-edge extensions) and movable leading-edge extensions (i.e., leading-edge vortex flaps) have been developed. Through extensive parametric studies on different experimental wing models, it has been shown that such devices, when properly designed and positioned, can confine the entire leading-edge vortices to the device upper surface and provide flow reattachment on the wing along the knee or hinge line.[5-10] As a result, the wing not only produces additional lift, but it also generates a thrust force components, as the low pressure associated with the confined vortices acts on the neighboring surfaces.

The objective of the present study is to develop a leading-edge device that can improve the aerodynamic performance and pitching moment characteristics of a thick swept-wing, cambered and twisted, high-subsonic, and low-supersonic aircraft at off-design conditions. This leading-edge device, designated as a leading-edge extention (LEE), is to be mounted to a wing along the dividing stream surface, called herein, the pseudo-stagnation stream surface (PSSS), associated with the attached flow design lift coefficient ($C_{L,d}>0$). (Note that $C_{L,d}=0$ work is reported in Ref. 11). The surface is called "pseudo" stagnation because, at its intersection with the wing, the velocity components are not all zero, except at the centerline. In fact, except at the centerline of a three-dimensional swept wing, there exists no other point on the wing surface, from a potential flow viewpoint, where zero sidewash (V_Y) will occur. The PSSS is a dividing stream surface that separates the incoming flow into two regimes, in general, over the upper and under the lower wing surfaces. Two streamwise cuts through the PSSS are shown schematically in Fig. 2 to illustrate the surface curvature.

The LEE is a portion of the PSSS and, if properly determined, should not affect the main wing aerodynamic performance at the attached flow design angle of attack (α_d). (Note that the angle of attack associated with $C_{L,d}$ is defined as α_d). This is illustrated by a streamwise cut through the LEE in Fig. 3a. However, at higher angles of incidence, vortices would be generated as a result of forced flow separation by the sharp leading edges of the LEE device. These vortices can be controlled through LEE planform shape optimization by varying parameters such as the chordwise extension, spanwise extension, and leading-edge sweep angle. A properly designed LEE planform can capture the entire leading-edge vortex on its upper surface and provide flow reattachment at, or near, the

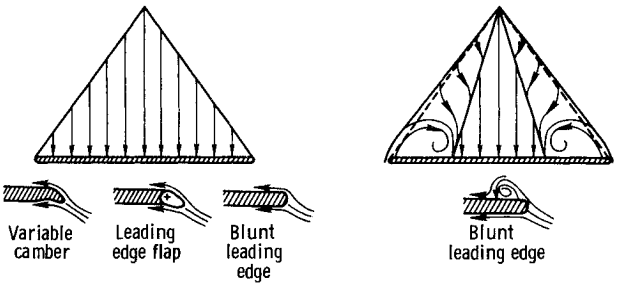

a) Attached flow (design condition) b) Vortex flow (off-design condition)

Fig. 1 Typical flow types occurring at the leading edges of an aircraft.

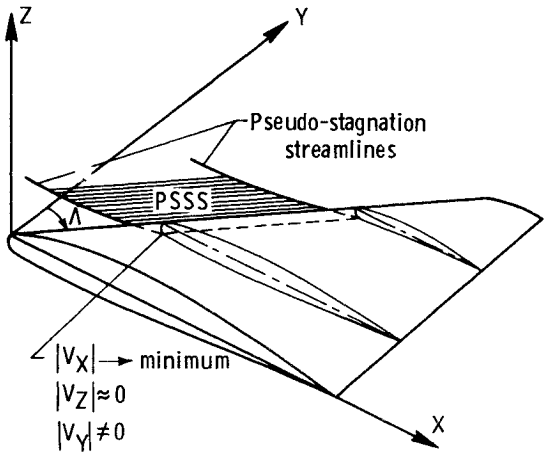

Fig. 2 Schematic representation of the PSSS corresponding to two wing sections.

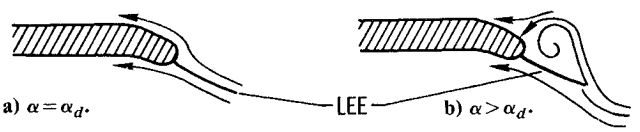

Fig. 3 Streamwise cut of flow about the leading edge of a wing + LEE combination.

wing upper surface leading edge (Fig. 3b). The confined leading-edge vortex system induces suction pressure that acts on the LEE upper surface and the forward-facing area of the wing leading edges, providing and additional lift and an effective leading-edge thrust recovery. As a result, the aerodynamic thrust force generated in the flight direction yields a reduction in drag, relative to a planar configuration, and the added lift permits the aircraft to operate at lower angles of attack that may delay pitch-up due to the improved trailing-edge flow. (Note: Skin-friction drag is ignored throughout this study.)

Design Procedure

In order to accomplish the task of designing an aerodynamically efficient LEE planform shape, an analytical procedure had to be developed. This design procedure, which forms the basis of the present study, can be outlined in two major steps:

1) Analytical determination of PSSS at the attached flow design condition for the wing.

2) Analytical optimization of the chordwise extent and the planform shape of the PSSS at separated flow conditions. This step would, in fact, determine the optimum LEE size for the given wing.

The final LEE is considered to be optimum in this study when the following criteria, which are referred to as the design requirements, are satisfied:

1) Its presence on the wing does not change the pressures and, therefore, the aerodynamic performance of the wing alone at the design lift coefficient.

2) The net lifting pressure across it approaches zero (target value) at the design lift coefficient.

3) It maintains a minimum planform area and chord length, especially in the tip region where and wing local chord becomes shorter.

4) Its intersection with the wing remains on the wing lower surface.

Analytical Tools

To demonstrate the design procedure outlined earlier, computer codes (i.e., analytical tools) and a candidate wing had to be selected. As a result, a thick, round-edge, twisted, and cambered wing of approximately triangular planform having a sweep of 58 deg and an aspect ratio of 2.3, was chosen to provide the first application of this technique. At the outset, four computer codes were considered for analytical execution of the present study at a high-subsonic Mach number. These codes were free vortex sheet code (FVS),[12] panel aerodynamics code (PAN AIR),[13] vortex lattice method with suction analogy code (VLM-SA),[14-16] and a transonic computer code. Although attempts were made to obtain and employ a nonlinear transonic computer code in this study, due to the high-subsonic Mach numbers of interest, none was available to the authors when this study began that could reliably estimate the pressures on thick delta wings. The FVS was not employed because of the first author's unsuccessful past experience, which included efforts to obtain a converged solution for the DM-1 with a leading-edge extension of Ref. 11.[17] Further valid flowfield results could not be obtained by the VLM-SA because of the lack of thickness modeling by the code.

The PAN AIR code was evaluated by modeling the candidate wing geometry using the flow conditions of interest. A pressure distribution obtained from the code is compared with experimental results and discussed in Appendix A. Hence, after the preliminary examination of the remaining code options, the PAN AIR was assigned to determine the PSSS and the VLM-SA code to establish the proper extent for the LEE. The use of the thin wing VLM-SA code to model thick wing, with and without LEE, is discussed in Appendix B. It should be noted that the theoretical impact of thickness and viscous effects on a thick wing configuration with LEE having vortical flow has yet to be addressed in the literature. Hence, the use of the VLM-SA is a first attempt to model a wide range of wing + LEE combinations in a short time in order to assess important geometrical influences on lift-to-drag ratio.

PSSS Determination

Assumptions

Part (1) of the two-part present study seeks to determine a representation of the PSSS based on the following assumptions:

1) There exists a PSSS associated with a swept-wing aircraft at the attached flow design condition.

2) The intersection of the PSSS with a number of parallel XZ planes spanning the wing produces curves that are representative of the pseudo-stagnation streamline (PSS) leading to the pseudo-stagnation point (i.e., $|V_X| \rightarrow$ minimum, $|V_Z| \approx 0$; note that $|V_Y|$ is not assumed to be small nor zero and is not treated in part 1 of this study).

3) The PSS shapes are derived from the local slopes of the resultant velocities $\sqrt{V_X^2 + V_Z^2}$ at appropriate points in the XZ plane.

4) A spanwise surface fitted linearly through the resulting intersections is an approximation of the PSSS described in the first assumption.

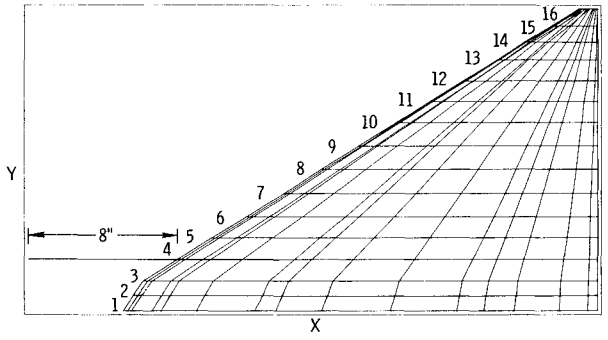

Fig. 4 Semispan planform view of the wing model with survey network located at fourth station. a) original panels, b) final panels.

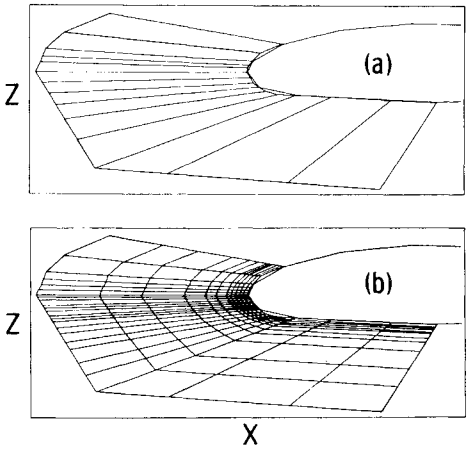

Fig. 5 Enlarged cross-sectional view at fourth station.

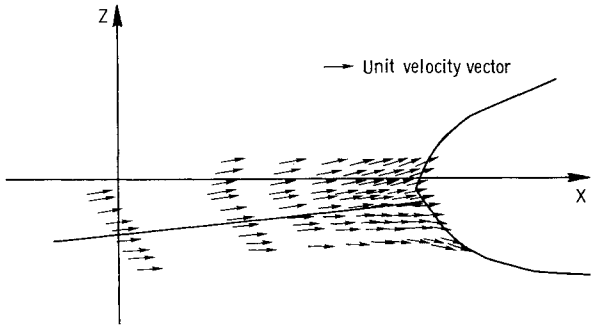

Fig. 6 Graphically determined PSS from typical section velocity field.

Part (2) of the present study shows how improvements can be made in the resulting LEE by including the influence of V_Y.

Survey Networks

The survey networks adopted in the present study were vertical XZ planes located at 16 different stations along the semispan of the wing model. These survey networks were generated such that each would enclose the nose portion of its corresponding station and stand off from the section a distance of approximately 0.08% of the wing c_r. The networks began at the upper surface just behind the leading edge and extended around the nose to the lower surface midchord. Due to the similarity of the survey network geometries and the involved process of their generation, only a typical survey network (located at the fourth station), shown in Fig. 4, will be discussed. This figure also shows the planform distribution of the other survey network locations over the semispan of the

wing model. Further, the enlarged cross-sectional view of the survey network and the nose portion of its corresponding wing section at the fourth station is shown in Fig. 5a.

Since the PAN AIR code velocity field solutions were assigned to be calculated at the center point of each panel in a particular survey network, it was essential to provide the survey networks with enough panels so that, once the resultant velocity vectors associated with V_X and V_Z were plotted, the pseudo-stagnation streamlines could be depicted graphically for each wing section. For this purpose, a geometrical computer code, called GEOMABS,[18] was employed to intensify the paneling on the survey networks. Figure 5b shows the repaneled survey network. It can be seen from the figure that the panel density is concentrated primarily around the portion of the survey network that faces the nose of the associated wing section. This provides more velocity vector solutions, which are needed to determine graphically the accurate location of the resulting pseudo-stagnation streamlines as they meet their corresponding wing section. Similar survey networks were generated for all 16 semispan stations of the wing model. Each individual survey network was positioned on the wing model and separate PAN AIR code execution was performed.

PAN AIR Analysis

The PAN AIR numerical representation of the studied thick delta wing consisted of three aerodynamic surfaces over the half-model. These surfaces, often referred to as networks, were explicitly associated with the wing upper and lower surface and the tip. Initially, the tip surface was not included because zero thickness was assumed there. However, this led to unrealistic solutions in the tip region. Hence, a small thickness was added at the tip to circumvent this problem. No-flow-through boundary conditions were employed on the exterior (wetted) surfaces along with zero perturbation potential in interior regions.

The PAN AIR task was successfully accomplished and the velocity field solutions for different wing sections were analytically determined at the attached flow design lift coefficient of 0.25 and Mach number of 0.8. (Note that the angle of attack associated with $C_{L,d}$ was 6.0 deg). Neglecting the sidewash V_Y effect, the resultant velocity vectors obtained from vectorial addition of the axial V_X and the upwash V_Z velocity components associated with each wing section were plotted. Further, the streamline associated with the minimum velocity magnitude (i.e., $|V_X| \rightarrow$ minimum, $|V_Z| \approx 0$, pseudo-stagnation point) was drawn tangent to the plotted velocity vectors. Figure 6 shows the nose portion of a typical airfoil section with its corresponding velocity field and the graphical PSS solution. These graphical streamline solutions yielded their coordinate point relative to the corresponding wing section. Each of these solutions was equally extended out a distance of 4.8 in. (i.e., 19% of wing c_r) ahead of the wing leading edge. This distance was thought to be sufficient to bracket the useful design space of a LEE device from an aerodynamic and structural viewpoint. Furthermore, it should be noted that the computed velocity field solutions obtained showed that the pseudo-stagnation point is occurring on the wing upper surface outboard of 89% semispan. This effect could well be due to the relatively high twist of the wing, which is more pronounced around the tip region. Hence, in order to maintain the wing-LEE intersection line on the wing lower surface (design requirement), neither the velocity field solutions nor the associated portion of the PSSS was sought over that portion of the span.

The warped PSSS was represented by fitting straight line segments through the available PSS solutions that ran roughly parallel to the wing leading edge. The three-view computer drawing of the determined PSSS solution is shown in Fig. 7. Futher, five cross-sectional cuts through the wing+PSSS combination and the enlarged cross-sectional view of the same cuts shown in Fig. 8. The resulting PSSS has approximately a

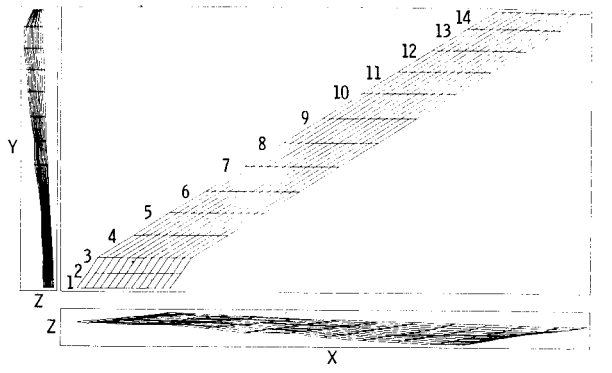

Fig. 7 Three views of the determined PSSS solution.

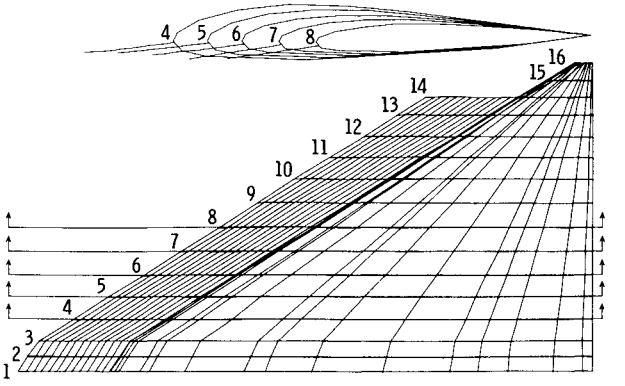

Fig. 8 Typical streamwise cuts through the wing+PSSS combination. a) wing, b)PSSS.

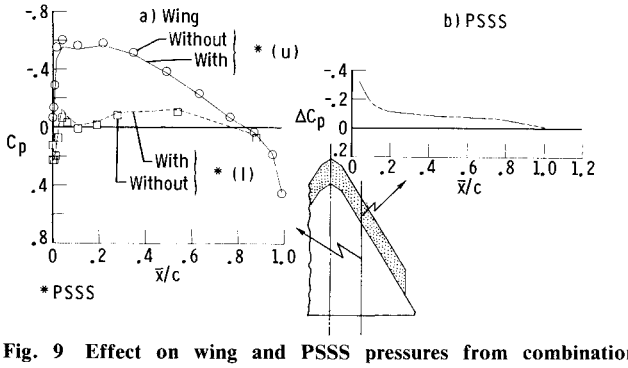

Fig. 9 Effect on wing and PSSS pressures from combination ($\eta = 0.34$, $\alpha_d = 6.0$ deg, $M_\infty = 0.8$)

14.33 in. semispan (i.e., 89% of the wing semispan) and 4.8 in. constant-chord extent.

It is essential to examine the degree of accuracy of the determined PSSS solution. For this purpose, the PAN AIR code was employed once again to model the wing+PSSS combination at the design condition (i.e., $\alpha_d = 6.0$ deg, $M_\infty = 0.8$) by specifying the PSSS at a lifting surface. Figure 9a shows the effect of the PSSS presence on the wing pressure distribution at a typical wing section to be insignificant. Also, as shown in Fig. 9b, the net lifting pressure across the PSSS appears small except at the local leading edge for the same typical section. From these results, it is evident that the addition of the PSSS surface does not cause much change in the performance of the wing model at the design condition. Therefore, it is concluded that the determined PSSS solution is close to the actual dividing stream surface (i.e., PSSS) and hence, it completes part (1) of the design procedure outlined earlier.

LEE Planform Optimization

Part (2) of the design procedure is performed by employing the VLM-SA code, which attempts to optimize the PSSS planform shape. This optimum shape is then designated as the shape of the LEE device. The aerodynamic effectiveness of 36 different LEE planform shapes was examined for the given wing by considering the influence of geometrical parameter choices such as constant chord (c_{LEE}), constant sweep (Λ_{LEE}), and span extent (η_{LEE}). The planform view of these parameters relative to the basic wing geometry is illustrated schematically in Fig. 10. Although the twist and camber of the basic wing is represented by its mean camber surface, the thickness effect is ignored by the VLM-SA code. As discussed in Appendix B, the analytical solution for the basic wing model, which was first intended to provide a baseline for comparative assessments of the LEE device, appears to be inadequate. As a result, throughout this study, the aerodynamic effectiveness of different wing + LEE combinations was emphasized more relative to one another rather than to the basic wing.

The VLM-SA drag polar solutions for the selected constant-chord and constant-sweep LEEs with 89% span extent are presented in Fig. 11. It is evident from this figure that considerable improvement can be achieved in the lift and drag characteristics of the wing + LEE combination by employing a longer LEE chord extension. However, as it was noted earlier, one design criterion for the final LEE planform was to satisfy a minimum chord length, especially in the tip region. A smaller chord LEE not only benefits from the reduced structural weight, but it also minimizes the effect of bending moment about the wing-LEE junction. The bending moment occurs at off-design conditions where the low pressure associated with the leading-edge vortices act on the upper surface of the LEE device.

It appears instructive to compare the aerodynamic effectiveness of different LEEs relative to their planform area by considering the effect of other geometrical parameters. For this purpose, Fig. 12 was prepared. In general, this figure shows that the LEE planform area does not have much effect on lift-to-drag ratio over the entire range of angle of attack. Further, with regard to the comparison of the aerodynamic effectiveness of LEEs with different constant chords and constant sweep angles, the following conclusions are drawn based on equal LEE planform area:

1) At moderate angles of attack (6-10 deg), it appears that constant-chord LEEs produce a better lift-to-drag ratio.

2) At 12 deg angle of attack, LEEs with constant sweep angles of 55-57 deg generate better L/D; however, outside this range, constant-chord LEEs achieve either the same or better improvements.

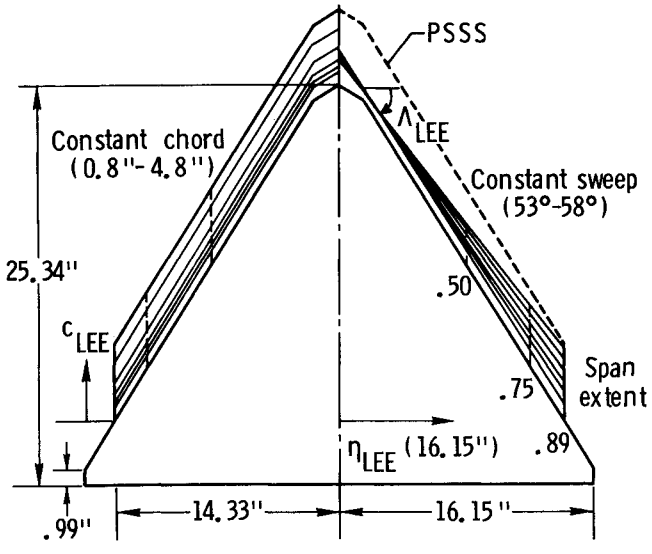

Fig. 10 LEE design parameters and ranges.

3) At 14-16 deg angle of attack, only low sweep angle LEEs appear to be more effective. However, at higher angles of attack (18-20 deg), Fig. 12 shows a very slight change in L/D ratio, regardless of the LEE's planform shape or area.

It should be noted that Fig. 12 also shows the available experimental data[20] for the basic wing (zero LEE area) at four different angles of attack (6, 8, 10 and 12 deg). These data appear to be the asymptotic values of the VLM-SA solution curves with decreasing LEE planform area. Obviously, this is the correct trend and is gratifying.

In general, this investigation revealed that, with the same planform area, constant chord is relatively more effective than LEEs having sweep angles less than that of the wing. Therefore, two LEE planforms, each with 89% span extent relative to the wing span, one with 1.2 in. and the other with 0.8 in. constant chord, were selected as being the best candidates for the final LEE design planform. These results, along with the aerodynamic effectiveness of other studied LEE geometrical parameters, have been reported in Ref. 19. Also, in the same reference, it has been shown that reducing the outboard extent of the LEE is directly related to a reduction in the lift-to-drag ratio, regardless of the LEE planform shape or area. This concludes the first part of the present study.

The second part was undertaken to improve the pressure distributions of the wing + LEE combination at α_d. For this purpose, the PAN AIR code was employed to model the basic wing with 1.2 in. constant-chord LEE having 89% span extent. As shown in Fig. 13a, the LEE presence appears to

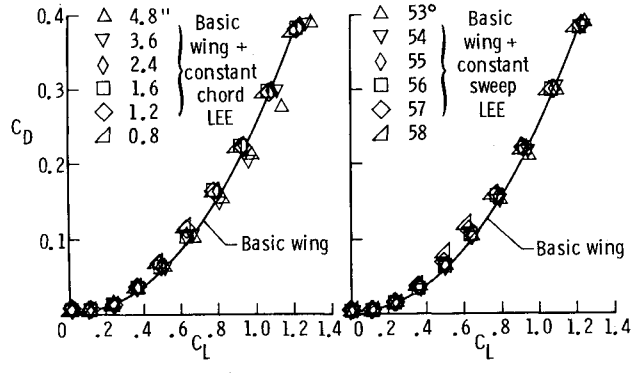

Fig. 11 Drag polar for constant chord and sweep variation ($\eta_{LEE} = 0.89$, $M_\infty = 0.8$).

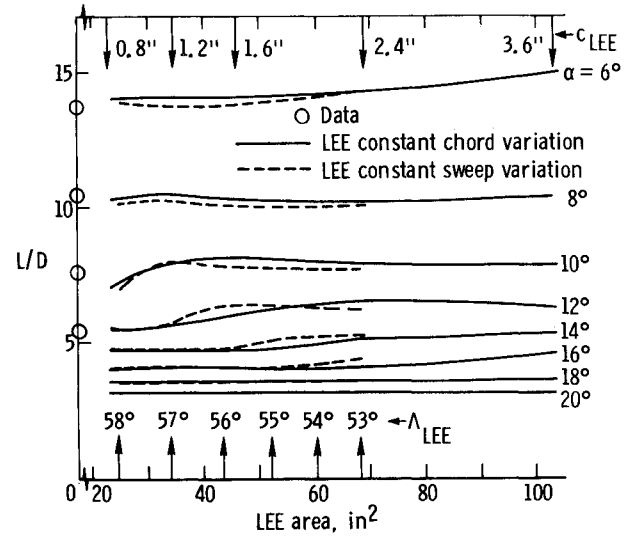

Fig. 12 Effect of LEE planform geometrical parameters on lift-to-drag ratio ($\eta_{LEE} = 0.89$, $M_\infty = 0.8$).

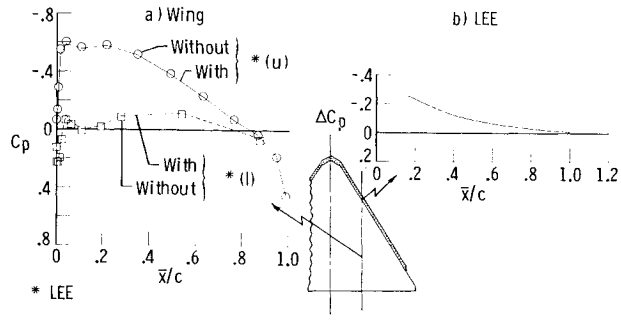

Fig. 13 Effect on wing and LEE pressures from combination ($\eta = 0.34$, $\alpha_d = 6.0$ deg, $M_\infty = 0.8$): a) wing, b) LEE.

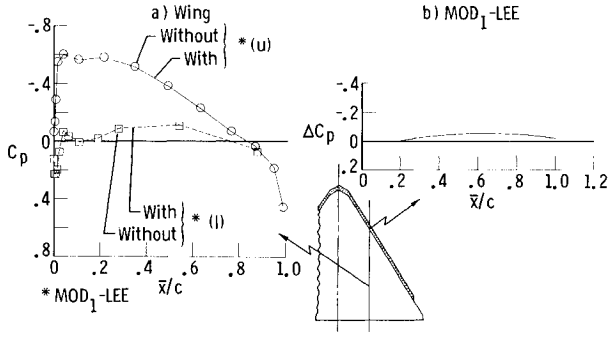

Fig. 14 Effect on wing and MOD_1-LEE pressures from combination ($\eta = 0.34$, $\alpha_d = 6.0$ deg, $M_\infty = 0.8$): a) wing, b) MOD_1 + LEE.

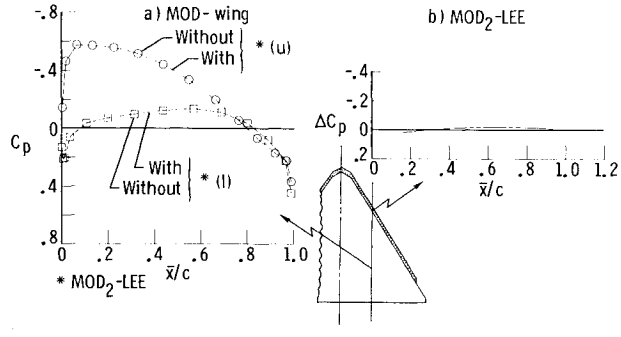

Fig. 15 Effect on modified and MOD_2-LEE pressures from combination ($\eta = 0.34$, $\alpha_d = 6.0$ deg, $M_\infty = 0.8$): a) modified wing, b) MOD_2-LEE.

disturb the pressure distribution slightly at the leading edge of the typical wing section. This effect indicates that perhaps the LEE surface is not completely aligned with the flow. In fact, the same effect is more obvious from the net lifting pressure across the LEE at the same typical section, as shown in Fig. 13b. Apparently, the LEE surface is generating some negative pressure on its upper surface, especially around its leading edge. This misalignment of the LEE surface with the incoming flow can be understood when the aerodynamic effects of the actual geometry being modeled is reconsidered. This examination points out a deficiency in one of the assumptions made in the PSSS determination (i.e., neglecting the effect of the sidewash velocity component). In particular, the spanwise connection of the graphically determine PSS with straight lines to represent the PSSS produces a different three-dimensional potential flow problem. Further, it is important to note that all the pressure distributions presented in this study are based on the second-order solutions where the sidewash effects are included.

Aerodynamic principles suggest that, in order to reduce the negative lifting pressure and to improve the flow characteristics at the LEE leading edge, the LEE surface must

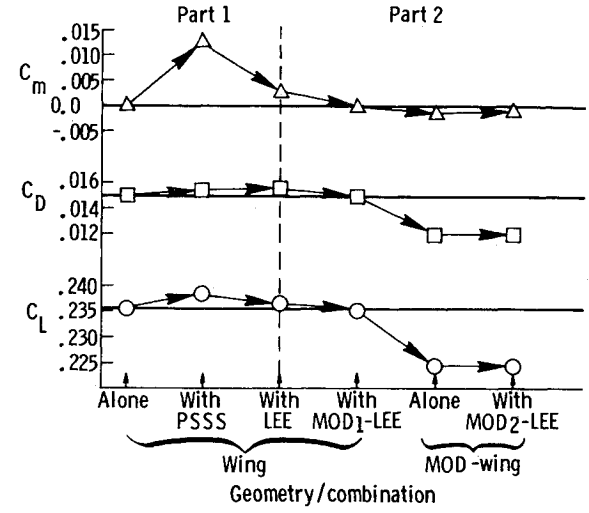

Fig. 16 PAN AIR solutions for wing alone and with LEE at $\alpha_d = 6.0$ deg.

be lowered. These principles were employed and the LEE surface was lowered by rotating it slightly (7 deg) while holding the pseudo-stagnation points fixed. Figure 14 shows the PAN AIR solutions for the modified LEE (MOD_1-LEE) geometry. This figure shows that by lowering the original LEE surface, the chordwise pressure distributions on the basic wing and across the LEE surface were improved.

The original wing geometry representation was determined to contain fictitious cavities that were subsequently removed by judicious smoothing. As a result, the PAN AIR code was employed once again to model the modified wing (MOD-wing) geometry. Furthermore, the MOD_1-LEE was slightly modified for the new wing geometry at α_d and is called MOD_2-LEE. As shown in Fig. 15, the chordwise pressure distribution at the same typical wing section appears to be insensitive to the LEE presence. This figure also shows the net lifting pressure across the LEE surface to be approximately zero (i.e., the target design value). The summary of the force and moment results obtained from PAN AIR code are presented in Fig. 16. This figure shows how well each different wing + LEE combination duplicate the wing-alone aerodynamic results at α_d. Thus, the previously described method has been shown to theoretically predict essentially no effect of the LEE at the design angle of attack.

Conclusions

The present study demonstrated the applicability of a newly developed analytical design procedure for the determination of a noninterferring leading-edge extension (LEE) that satisfies certain design criteria for thick delta wings. This procedure led to a successful estimation of the shape of the LEE device, which is a portion of the pseudo-stagnation stream surface, that had essentially no effect on the wing-alone aerodynamic results at its design angle of attack. Through an examination of the available analytical tools, the PAN AIR and VLM-SA computer codes were employed to carry out the first application of the developed design procedure for the given wing of the present study.

The results obtained for 36 different LEE planforms suggest that 1.2 and 0.8 in. constant chord with 89% span extent satisfy the constraints (i.e., design criteria) and are considered good candidates for the final LEE planform design. Although efforts have been made to validate the results obtained in the present study whenever possible, these results need to be verified experimentally.

Appendix A: PAN AIR Evaluation

The intended purpose of this appendix is to evaluate the analytical capability of the PAN AIR code for thick wing configurations at high Mach numbers of interest. As a result, the

thick wing geometry of the present study was modeled with PAN AIR code at $\alpha_d = 6.0$ deg and $M_\infty = 0.8$. the pressure distribution obtained by the code is compared with experimental[21] data at $\eta = 0.30$ in Fig. A1. The comparison shows good agreement between the theoretical and experimental data except on the forward part of the upper surface. The difference may be due to either differences in geometry (sting shroud omitted in PAN AIR) or flow types between the experimental configuration and theoretical modeling.

Appendix B: VLM-SA Evaluation

As part of the present study, it was important to examine the analytical capability of the VLM-SA code for a thick wing configuration with a leading-edge extension. For this purpose, the experimental data obtained by Wilson and Lovell[11] on the thick DM-1 with and without the LEE was selected for validating the results obtained from the VLM-SA code. The DM-1 is a symmetrical wing configuration with an airfoil section like the NACA 0015-64 and no twist, so the LEE design lift coefficient ($C_{L,d}$) was zero. Although the effect of leading-edge radii is included in the resulting VLM-SA solutions, the thick DM-1 is approximated by its projected planform (flat DM-1) in this study.

Experimental values for the lift and drag polars obtained by Wilson and Lovell for the DM-1 with and without the LEE, as well as the resulting VLM-SA solutions for the same configurations, are presented in Fig. B1 C_{D_0} from Ref. 11 were added to VLM-SA solutions.) Obviously, the code overestimated the lift for both the DM-1 and DM-1 + LEE combination throughout the angle-of-attack range. However, the polar comparison shows that, for the basic DM-1, the VLM-SA solutions have the same variation as the experimental data up to $C_L = 0.6$. Beyond this lift coefficient, the curves differ due to the disorganized flow over the basic DM-1, which causes both a drag increase and lift decrease.[11] As a result, the experimental drag polar is higher than the theoretical solution. For the DM-1 + LEE combination, the VLM-SA over estimates the drag in the lift coefficient range of about 0.05-0.80. This difference was rather expected, because the resulting VLM-SA solutions do not include the effect of the low pressures acting between the LEE and upper surface maximum thickness line of the wing section to produce a thrust. Hence, the computed C_D values are higher than the experimental data. Therefore, by analogy, it is expected that the VLM-SA solution for the drag would be higher in the wing + LEE analysis of the present study than the experimental data.

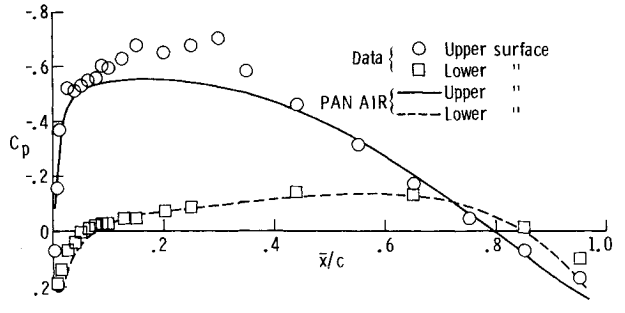

Fig. A1 Experimental and theoretical pressures for the modified wing ($\eta = 0.30$, $\alpha_d = 6.0$ deg, $M_\infty = 0.8$).

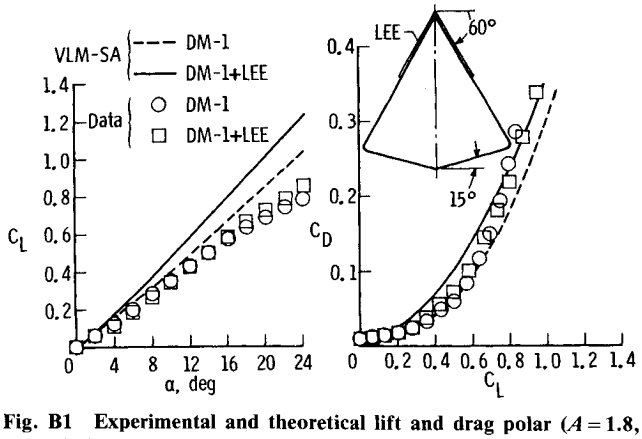

Fig. B1 Experimental and theoretical lift and drag polar ($A = 1.8$, $M_\infty = 0.0$).

References

[1]Wentz, W.H. Jr., "Effects of Leading-Edge Camber on Low-Speed Characteristics of Slender Delta Wings," NASA CR-2002, Oct. 1972.

[2]Rao, D.M., "Exploratory Subsonic Investigation of Vortex Flap Concept on Arrow Wing Configuration," NASA CP-2108 (Pt. 1), Nov. 1979.

[3]Henderson, W.P., "Effects of Wing Leading-Edge Radius and Reynolds Number on Longitudinal Aerodynamic Characteristics of Highly Swept Wing-Body Combinations at Supersonic Speeds," NASA TN D-8361, Dec. 1976.

[4]Bobbitt, P.J., "Modern Fluid Dynamics of Subsonic and Transonic Flight," AIAA Paper 80-0861, May 1980.

[5]Rao, D.M., "Leading-Edge Vortex Flaps for Enhanced Subsonic Aerodynamics of Slender Wings," ICAS 80-13.5, Oct. 1980.

[6]Johnson, T.D., Jr. and Rao, D.M., "Experimental Study of Delta Wing Leading-Edge Devices for Drag Reduction at High Lift," NASA CR-165846, Feb. 1982.

[7]Tingas, S.A. and Rao, D.M., "Experimental Balance and Pressure Investigation of a 60° Delta Wing with Leading-Edge Devices," NASA CR-165923, May 1982.

[8]Yip, L.P. and Murri, D.G., "Effects of Vortex Flaps on the Low-Speed Aerodynamic Characteristics of an Arrow Wing," NASA TP-1914, Nov. 1981.

[9]Rao, D.M., "Leading-Edge Vortex Flap Experiments on a 74° Delta Wing," NASA CR-159151, Nov. 1979.

[10]Lamar, J.E. and Campbell, J.F., "Recent Studies at NASA Langley of Vortical Flow Interacting with Neighboring Surfaces," Paper 10 presented at AGARD Symposium on Aerodynamic of Vortical Type Flows in Three-Dimensions, April 1983.

[11]Wilson, H.A. Jr and Lovell, J.C., "Full-Scale Investigation of the Maximum Lift and Flow Characteristics of an Airplane Having Approximately Triangular Planforms," NASA TM No. L6K20, Feb. 1947.

[12]Johnson, F.T., Lu, P., Tinoco, E.N., and Eption, M.A., "An Improved Panel Method for the Solution of Three-Dimensional Leading-Edge Vortex Flows," NASA CR-159173, June 1979.

[13]Sidwell, K.W., Baruah, P.K., and Bussoletti, J.E., "PAN-AIR A Computer Program for Predicting Subsonic or Supersonic Linear Potential Flows about Arbitrary Configurations Using a Higher Order Panel Method," NASA CR-3252, May 1980.

[14]Lamar, J.E. and Gloss, B.B., "Subsonic Aerodynamic Characteristic of Interacting Lifting Surfaces with Separated Flow Around Sharp Edges Predicted by a Vortex Lattice Method," NASA TN D-7921, Sept., 1875.

[15]Lamar, J.E. and Herbert, H.E., "Production Version of the Extended NASA-Langley Vortex Lattice FORTRAN Computer Program, Vol. I: Source Code," NASA TM-83303, April 1982.

[16]Herbert, H.E. and Lamar, J.E., "Production Version of the Extended NASA-Langley Vortex Lattice FORTRAN Computer Program, Vol. II: Source Code," NASA TM 83304, April 1982.

[17]Chaturvedi, S.K. and Ghaffari, F., "An Investigation of Aerodynamic Characteristics of Wings Having Vortex Flow Using Different Numerical Codes," Old Dominion University Research Foundation, Norfolk, VA, Final Report, Research Grant NSG-1561, April 1984.

[18]Hall, J.F., Neuhart, D.H., and Walkley, K.B., "An Interactive Program for Manipulation and Display of Panel Method Geometry," NASA CR-166098, March 1983.

[19]Ghaffari, F. and Chaturvedi, S.K., "An Analytical Design Procedure for the Determination of Effective Leading-edge Extensions on Thick Delta Wings," NASA CR-172351, May 1984.

[20]Chu, J., Lamar, J.E., and Luckring, J.M., "Longitudinal Test and Evaluation of Six 58° Cambered and Twisted Thick Delta Wings at High Subsonic Speeds," NASA TM-85786, March 1985.

[21]Chu, J. and Lamar, J.E., "Summary of a High Subsonic Fore/Pressure Experiment for 58° Cambered/Twisted Thick Delta Wings," AIAA Paper 86-0169, Jan. 1986.